Inorganica Chimica Acta 375 (2011) 106–113

Contents lists available at ScienceDirect

Inorganica Chimica Acta

journal homepage: www.elsevier.com/locate/ica

# Synthesis, crystal structure, and catalytic studies on dinuclear copper(II) mesocates

P. Mosae Selvakumar [a], Sandeep Nadella [a], K. Jeya Prathap [b], R.I. Kureshy [b], E. Suresh [a], P.S. Subramanian [a,*]

[a] *Analytical Science Division, Central Salt and Marine Chemicals Research Institute (CSIR), G.B. Marg, Bhavnagar 364 002, Gujarat, India*
[b] *Discipline of Inorganic Materials and Catalysis, Central Salt and Marine Chemicals Research Institute (CSIR), G.B. Marg, Bhavnagar 364 002, Gujarat, India*

ARTICLE INFO

*Article history:*
Received 28 January 2011
Received in revised form 29 March 2011
Accepted 20 April 2011
Available online 28 April 2011

*Keywords:*
Copper(II)
Crystal structure
Catalysis
Helicates
Henry reaction
Schiff base

ABSTRACT

Imine based bis-bidentate ligands $H_2$-*m*-xysal, ($L_1H_2$); $H_2$-*m*-xysal-Cl, ($L_2H_2$); $H_2$-*m*-xysal-Br, ($L_3H_2$); $H_2$-*m*-xysal-$OCH_3$, ($L_4H_2$); $H_2$-*m*-xysal-(*t*-Bu)$_2$, ($L_5H_2$) were synthesized and characterized. These substituted 1,3-bis(hydroxylbenzyl)-diaminoxylene dianion ligands upon treating with copper(II) acetate in 2:2 equivalent of L:M ratio, resulted in a series of binuclear [$Cu_2$(*m*-xysal)$_2$] neutral complexes **1**–**5**. The crystal structures determined for the complexes **1** and **2** indicate a dinuclear association. The CH···π interaction observed between the metal-chelate ring and the hydrogens associated with *m*-xylene spacer moiety being first in this series of complexes, is demonstrated to stabilize the helical conformation through intramolecular self assembly process. The position of the resonance on the EPR spectra and the absence of $\Delta Ms = \pm 1$ feature for the complexes **2**, **3**, and **5** obtained for room temperature solid state samples revealed that the metal centers though exist in the dinuclear unit, they are separated from each other and possess a non-interacting monomer-type metal–metal association. The Cu(II) centers in all these complexes possessing an intermediate geometry between tetrahedral and square planar, an appropriate catalytic study converting 4-nitrobenzaldehye to corresponding nitroaldol was carried out using complex **5**.

## 1. Introduction

Copper(II), an active site in several metalloproteins [1,2] and metalloenzymes, is known to form complexes with variety of molecular geometries [3] e.g. tetrahedral, square planar, square pyramidal, and octahedral. Cu(II) in blue copper proteins possessing an intermediate geometry between the tetrahedral and square planar, several model systems including those with bidentate Schiff base ligands had been reported for their structure–functional activity [4–7]. Similarly, helicity [8] plays vital role on various biocomponents, such as enzymes, proteins, DNA, and α-amylase, etc. Helicates thus gained paramount importance due to their unique architectural aspect and hence the reports on varieties of helicates [8–11] comprising single, double, triple, and multi-strands are rich in the recent decade. Though the reports on helicates are rich, researchers are yet to recognize some of their promising applications [12].

The helicates, thus possessing both helical conformation and Cu(II) active centers, hold immense interest. Further, the helical conformation influenced by various supramolecular interactions and the consequent changes in the geometry are considered to be important in view of their catalytic role [13,14]. In this direction though there are many metallohelicates, the preparation of αα′-bis(salicylidinine)xylene as a mixture of *meta* and *para* isomer reported by Yoshida et al. [15,16] and McNelis et al. [17] gained significance. In continuation of that, Reedijk and coworkers [18] have reported recently, the solution state studies along with its crystal structures. Similarly, incorporating the isostructural spacer, i.e., *m*-phenylenediamine(sal-$PDAH_2$) and the *m*-xylenediamine [$H_2$-*m*-xysal], the respective bis(2-hydroxybenzoyl)diamino benzene Schiff base ligands and dinuclear [$Cu_2$(*m*-xysal)$_2$] complexes were already reported. In this regard the present study reports the synthesis of a series of bis-bidentate Schiff-base ligands composed with *m*-xylene spacer moiety and their respective binuclear Cu(II) double helicates. While all these ligands and their Cu(II) helicates are characterized using various spectroscopic techniques, the crystal structures obtained for the complexes **1** and **2** are discussed in detail. In this direction the reports by Potts [19–21], Constable and coworkers [22–24] and Lehn [25,26] though demonstrated some interesting Cu(I) and Cu(II) helicates, those studies with polypyridyl ligands differ from the simple imine ligands used in the present study. The coexistence of both the helical conformation and the Cu(II) geometry with tetrahedrally distorted square planar geometry preserves an added advantage in view of catalysis. In addition, copper being catalytically important among the metals used in the henry catalysts, it's low cost, low toxicity and wide utility in varieties of organic reactions, inspired us to examine their

---

* Corresponding author. Tel.: +91 278 2567760; fax: +91 278 2567562.
*E-mail addresses:* siva@csmcri.org, siva140@yahoo.co.in (P.S. Subramanian).

0020-1693/$ - see front matter © 2011 Elsevier B.V. All rights reserved.
doi:10.1016/j.ica.2011.04.033

catalytic activity. Accordingly the catalytic investigation using the complex **5** as representative catalyst was carried out following the standard protocol used for nitroaldol catalysis (Henry reaction) [27]. Further the detailed study on the CH···π (metal-chelate ring) interaction and its influence on the helical conformation involving in tuning the Cu(II) geometry is also discussed in the present report.

## 2. Experimental

### 2.1. Materials and general methods

All the chemicals were purchased from Aldrich & Co. Microanalysis of the complexes was done using a Perkin-Elmer PE 2400 series II CHNS/O elemental analyzer. IR spectra were recorded using KBr pellets (1% w/w) on a Perkin-Elmer Spectrum GX FT-IR spectrophotometer. Electronic spectra were recorded on a Schimadzu UV 3101PC spectrophotometer. Mass analyses were performed using positive electron spray ionization ($ESI^+$) technique on a waters Q Tof-micro mass spectrometer for all these complexes upon dissolving in 50:50 $CH_2Cl_2$:$CH_3OH$ solvent mixture. $^1H$ NMR spectra were recorded on a Bruker Avance II 200 FT-NMR spectrometer. Chemical shifts for proton resonances are reported in ppm ($\delta$) relative to tetramethyl silane. Electron spin resonance spectra were recorded using Bruker X-band electron paramagnetic resonance spectrometer. The formation of nitroaldol was determined by HPLC (Shimadzu SCL-10AVP) using Chiracel columns (AD, OD, OD-H).

### 2.2. X-ray crystallography

In each case, a crystal of suitable size was selected from the mother liquor and immersed in partone oil, then mounted on the tip of a glass fiber, and cemented using epoxy resin. Intensity data for all three crystals were collected using Mo Kα ($\lambda$ = 0.71073 Å) radiation on a Bruker SMART APEX diffractometer equipped with CCD area detector. The data integration and reduction were processed with SAINT [28] software. An empirical absorption correction was applied to the collected reflections with SADABS [29] using XPREP. The structures were solved by using SHELXTL [30] program and refined on $F^2$ by the full-matrix least-squares technique using SHELXL [31]. Graphics were generated using ORTEP and packing and H-bonding diagrams by PLATON [32] and MERCURY [33]. In all the three complexes, non-hydrogen atoms were refined anisotropically till convergence was reached and hydrogen atoms attached to all carbon atoms were geometrically fixed.

### 2.3. General procedure for Henry reaction

Nitroaldol reactions were carried out in a magnetically stirred screw cap vials. Copper (II) complex **5** was *in situ* generated by mixing $L_5H_2$ (0.1 mmol) with copper acetate (0.1 mmol) in THF (0.5 ml) at rt for 3 h and then appropriate aldehyde (1 mmol) and nitromethane (1 mmol) were added to the resulting brownish solution which was allowed to stir continuously for 35–48 h at rt to 75 °C. The completion of the reaction was monitored by TLC. The product was purified by column chromatography by using *n*-hexane/EtOAc (90:10) ratio and confirmed by HPLC (Supplementary Fig. S4).

### 2.4. Synthesis

#### 2.4.1. Preparation of ligands

*2.4.1.1. General procedure.* Methanolic solution (75 ml) of aldehyde (0.002 mol) and 1,3-bis-amino methyl benzene (0.001 mol) were mixed and allowed for constant stirring with gentle heating for 3 h and then cooled to room temperature. The characteristic yellow precipitate obtained by Schiff base condensation reaction was filtered out. The yellow powder was dissolved in methanol:chloroform solvent mixture and allowed for slow evaporation at room temperature and the resultant dark yellow polycrystals were collected after 48 h.

*($H_2$-m-xysal) ($L_1H_2$).* 2,2′-(1,3-Phenylenebis (methylene))bis(azan-1-yl-1-ylidene)bis(methan-1-yl-1-ylidene)diphenol. Yield (90%). *Anal.* Calc. for $C_{22}H_{20}N_2O_2$; C, 76.72; H, 5.85; N, 8.13. Found: C, 76.61; H, 5.75; N, 86.18%. ESI-MS: Calc. for $C_{22}H_{20}N_2O_2$ $(M+H)^+$ 345.16. Found: 345.56; $^1H$ NMR ($CD_3CN$, $\delta$, 200 MHz): 13.37 (*Br s*, *–OH*, *2H*), 8.53 (s, *CH═N*, 2H), 7.36–7.23 (*m*, *Ar phenyl*, *8H*), 6.92–6.83 (*m*, *Ar*, *4H*), 4.75 (*s*, *N–CH*$_2$, *4H*). $^{13}C$ NMR (50 MHz, $CD_3CN$): 62.5($CH_2$), 116.5(CH), 118.7(CH), 126.8(CH), 127.4(CH), 129.0(C), 131.8(CH), 132.3(CH), 139.2 (C), 160.9(C–O), 166.4(CH═N). IR Spectra: ($\nu$, $cm^{-1}$) 3405, 3062, 2647, 1724, 1610, 1511, 1444, 1403, 1373, 1286, 1251, 1130, 754.

*($H_2$-m-xysal-Cl) ($L_2H_2$).* 2,2′-(1,3-Phenylenebis (methylene))bis(azan-1-yl-1-ylidene)bis(methan-1-yl-1-ylidene)bis(4-chlorophenol). Yield (96%). *Anal.* Calc. for $C_{22}H_{18}Cl_2N_2O_2$; C, 63.93; H, 4.39; N, 6.78. Found: C, 63.81; H, 4.38; N, 6.69%. ESI-MS: Calc. for $C_{22}H_{18}Cl_2N_2O_2$ $(M+H)^+$ 413.08. Found: 413.38; $^1H$ NMR ($CDCl_3$, $\delta$, 200 MHz): 13.31 (*Br s*, *–OH*, *2H*), 8.35 (s, *CH═N*, 2H), 7.39–7.21 (*m*, *Ar phenyl*, *6H*), 6.92–6.87 (*m*, *Ar*, *4H*), 4.80 (*s*, *N–CH*$_2$, *4H*). $^{13}C$ NMR (50 MHz, $CDCl_3$): 63.0($CH_2$), 118.6(CH), 119.5(C–Cl), 123.2(C), 127.0(CH), 129.2(CH), 130.5(CH), 132.2(CH), 138.2(C), 159.6(C–O), 164.5(CH═N). IR Spectra: ($\nu$, $cm^{-1}$) 3433, 3020, 2904, 1613, 1515, 1450, 1414, 1370, 1311, 1240, 1165, 1130, 1034, 980, 871, 820.

*($H_2$-m-xysal-Br) ($L_3H_2$).* 2,2′-2,2′(1,3-Phenylenebis (methylene))bis(azan-1-yl-1-ylidene)bis(methan-1-yl-1-ylidene)bis(4-bromophenol). Yield (95%). *Anal.* Calc. for $C_{22}H_{18}Br_2N_2O_2$; C, 52.62; H, 3.61; N, 5.58. Found: C, 52.64; H, 3.58; N, 5.51%. ESI-MS: Calc. for $C_{22}H_{18}Br_2N_2O_2$ $(M+H)^+$ 500.98. Found: 500.88; $^1H$ NMR ($CDCl_3$, $\delta$, 200 MHz): 13.35 (*Br s*, *–OH*, *2H*), 8.35 (s, *CH═N*, 2H), 7.41–7.21 (*m*, *Ar phenyl*, *6H*), 6.88–6.83 (*m*, *Ar*, *4H*), 4.81 (*s*, *N–CH*$_2$, *4H*). $^{13}C$ NMR (50 MHz, $CDCl_3$): 63.0($CH_2$), 110.0(C–Br), 119.0(CH), 120.0(C), 127.0(CH), 129.2(CH), 133.5(CH), 135.0(CH), 138.2(C), 160.1(C–O), 164.4(CH═N). IR Spectra: ($\nu$, $cm^{-1}$) 3420, 3058, 2640, 1718, 1617, 1515, 1450, 1400, 1365, 1270, 1230, 1118, 830.

*($H_2$-m-xysal-$OCH_3$) ($L_4H_2$).* 2,2′-6,6′(1,3-Phenylenebis(methylene))bis(azan-1-yl-1-ylidene)bis(methan-1-yl-1-ylidene)bis(2-methoxy phenol). Yield (90%). *Anal.* Calc. for $C_{26}H_{28}N_2O_4$; C, 72.20; H, 6.53; N, 6.48. Found: C, 72.11; H, 6.39; N, 6.32%. ESI-MS: Calc. for $C_{24}H_{24}N_2O_4$ $(M+H)^+$ 433.21. Found: 433.35; $^1H$ NMR ($CDCl_3$, $\delta$, 200 MHz): 15.55 (*Br s*, *–OH*, *2H*), 7.35–7.06 (*m*, *Ar phenyl*, *6H*), 6.97–6.84 (*m*, *Ar*, *4H*), 4.79 (*s*, *N–CH*$_2$, *4H*), 3.78 (*s*, *O–CH*$_3$, *6H*), *2.38* (*s*, *C–CH*$_3$, *6H*). $^{13}C$ NMR (50 MHz, $CDCl_3$): 15($CH_3$), 53.7 (O–$CH_3$), 56.1($CH_2$), 112.8(CH), 118.8(CH), 119.1(CH), 126.3(CH), 129.1(C), 139.1(C), 150.9(C–$OCH_3$), 157.3(C–O), 171.7(C═N). IR Spectra: ($\nu$, $cm^{-1}$) 3430, 3018, 2901, 1610, 1517, 1458, 1423, 1384, 1316, 1243, 1209, 1174, 1131, 1037, 989, 875.

*($H_2$-m-xysal-t-Bu) ($L_5H_2$).* 2,2′-6,6′(1,3-Phenylenebis (methylene))bis(azan-1-yl-1-ylidene)bis(methan-1-yl-1-ylidene)bis(2,4-di-tert-butylphenol). Yield (92%). *Anal.* Calc. for $C_{38}H_{52}N_2O_2$; C, 80.24; H, 9.21; N, 4.92. Found: C, 80.11; H, 9.16; N, 4.87%. ESI-MS: Calc. for $C_{38}H_{52}N_2O_2$ $(M+H)^+$ 569.41; Found: 569.70; $^1H$ NMR ($CDCl_3$, $\delta$, 200 MHz): 13.71 (*Br s*, *–OH*, *2H*), 8.46 (s, *CH═N*, 2H), 7.38–7.11 (*m*, *Ar phenyl*, *8H*), 4.78 (*s*, *N–CH*$_2$, *4H*), 1.43 (*s*, *C–CH*$_3$, *18H*)), *1*.30 (*s*, *C–CH*$_3$, *18H*). $^{13}C$ NMR (50 MHz, $CDCl_3$): 30.3($CH_3$), 32.4($CH_3$), 35.0(C), 35.9(C), 64.1($CH_2$), 118.8(C), 126.9(CH), 127.8(CH), 127.9(CH), 128.3(CH), 129.9(CH), 137.6(C), 139.7(C), 141.0(C), 159.2(C–O), 167.7(CH═N). IR Spectra: ($\nu$, $cm^{-1}$) 3400, 3070, 2655, 1732, 1618, 1515, 1430, 1415, 1370, 1290, 1242, 1127, 842.

### 2.5. Preparation of complexes

#### 2.5.1. General procedure

To the $H_2$-*m*-xysal ligand (0.001 mmol) dissolved in chloroform, an ethanolic solution of $[Cu(CH_3COO)_2{\cdot}H_2O]$ (0.001 mmol) was added drop by drop and allowed for constant stirring. During the course of the reaction a color change from yellow to dark brownish red indicate the formation of metal complex. In the case of complexes **1** and **2**, upon slow evaporation at room temperature, the dark brown crystals were obtained in 48 h.

*2.5.1.1. $[Cu_2(m\text{-}xysal)_2]{\cdot}EtOH$ (**1**).* Yield (87%). *Anal.* Calc. for $C_{46}H_{42}Cu_2N_4O_5$; C, 64.40; H, 4.93; N, 6.53. Found: C, 64.29; H, 4.87; N, 6.46%. ESI-MS: Calc. for $C_{44}H_{36}Cu_2N_4O_4$ $(M+H)^+$ 811.14. Found: 811.47; $(M+Na)^+$ 835.12 (835.47); UV–Vis [$CH_2Cl_2$, $\lambda_{max}$, nm, ($\varepsilon$, $M^{-1}\,cm^{-1}$)]: 257(36 726), 306(12 610), 385(13 045), 600(338). IR Spectra: ($\nu$, $cm^{-1}$): 3023, 2916, 1619, 1537, 1468, 1447, 1400, 1326, 1227, 1199, 1149, 10 951, 1037, 991, 905, 852.

*2.5.1.2. $[Cu_2(m\text{-}xysal\text{-}Cl)_2]$ (**2**).* Yield (90%). *Anal.* Calc. for $C_{44}H_{32}Cu_2Cl_4N_4O_4$; C, 55.65; H, 3.40; N, 5.90. Found: C, 55.58; H, 3.31; N, 5.81%. ESI-MS: Calc. for $C_{44}H_{32}Cu_2Cl_4N_4O_4$ $(M+H)^+$ 950.66. Found: 951.05; UV–Vis [$CH_2Cl_2$, $\lambda_{max}$, nm, ($\varepsilon$, $M^{-1}\,cm^{-1}$)]: 255(36 480), 306(19 980), 385(20 092), 625(430). IR Spectra: ($\nu$, $cm^{-1}$) 3025, 2908, 1622, 1524, 1458, 1423, 1384, 1316, 1243, 1209, 1174, 1131, 1037, 989, 875, 823.

*2.5.1.3. $[Cu_2(m\text{-}xysal\text{-}Br)_2]$ (**3**).* Yield (89%). *Anal.* Calc. for $C_{44}H_{32}Cu_2Br_4N_4O_4$; C, 46.87; H, 2.86; N, 4.97. Found: C, 46.74; H, 2.81; N, 4.79%. ESI-MS: Calc. for $C_{44}H_{32}Cu_2Br_4N_4O_4$ $(M+Na)^+$, 1150.76. Found: 1150.61; $(M+H)^+$, 1126.78(1126.65). UV–Vis [$CH_2Cl_2$, $\lambda_{max}$, nm, ($\varepsilon$, $M^{-1}\,cm^{-1}$)]: 260(36 550), 306(20 433), 390(23 047), 630(410). IR Spectra: ($\nu$, $cm^{-1}$) 3062, 2647, 1724, 1618, 1530, 1444, 1403, 1373, 1286, 1251, 1130, 750.

*2.5.1.4. $[Cu_2(m\text{-}xysal\text{-}OCH_3)_2]$ (**4**).* Yield (94%). *Anal.* Calc. for $C_{48}H_{44}Cu_2N_4O_8$; C, 63.21; H, 5.30; N, 5.67. Found: C, 63.17; H, 5.28; N, 5.56%. ESI-MS: Calc. for $C_{48}H_{44}Cu_2N_4O_8$ $(M+H)^+$ 989.09. Found: 989.30; UV–Vis [$CH_2Cl_2$, $\lambda_{max}$, nm, ($\varepsilon$, $M^{-1}\,cm^{-1}$)]: 270(36 600), 304(14 780), 367(18 090), 620(364). IR Spectra: ($\nu$, $cm^{-1}$) 3058, 2645, 1729, 1628, 1538, 1440, 1400, 1371, 1284, 1250, 1127, 740.

*2.5.1.5. $[Cu_2(m\text{-}xysal\text{-}t\text{-}Bu)_2]$ (**5**).* Yield (96%). *Anal.* Calc. for $C_{76}H_{100}Cu_2N_4O_4$; C, 72.40; H, 7.99; N, 4.44. Found: C, 72.31; H, 7.78; N, 4.39%. ESI-MS: Calc. for $C_{76}H_{100}Cu_2N_4O_4$ $(M+H)^+$ 1259.64. Found: 1260.71; UV–Vis [$CH_2Cl_2$, $\lambda_{max}$, nm, ($\varepsilon$, $M^{-1}\,cm^{-1}$)]: 260(36 580), 318(19 800), 385(19 950), 660(392). IR Spectra: ($\nu$, $cm^{-1}$) 3070, 2647, 1720, 1632, 1540, 1438, 1403, 1373, 1286, 1254, 1135, 754.

## 3. Results and discussion

The dianion ligands $L_1H_2$–$L_5H_2$ shown in Scheme 1 were prepared following imine condensation between the substituted salicylaldehydes and 1,3-bis-aminomethylbenzene. Keeping the *m*-xylene spacer moiety same, the ligands $L_1H_2$, $L_2H_2$, and $L_3H_2$ were obtained with appropriate aldehydes such as 2-hydroxybenzaldehyde, 2-hydroxy-5-chloro-benzaldehyde, and 2-hydroxy-5-bromo-benzaldehyde, respectively. Similarly, the ligands $L_4H_2$ and $L_5H_2$ were obtained upon treating *m*-xylenediamine with 2-hydroxy-3-methoxy-acetophenone and 2-hydroxy-3,5-di-*tert*-butyl-benzaldehyde, respectively. The Schiff base ligands $L_1H_2$–$L_5H_2$ are yellow in color and are soluble in various organic solvents, such as dichloromethane, chloroform, acetone, DMF, and DMSO. Upon adapting this series of ligands with copper(II)acetate in 2:2 metal:ligand ratio, a series of binuclear $Cu_2$ complexes $[Cu_2(L_1)_2]{\cdot}EtOH$ **1**, $[Cu_2(L_2)_2]$ **2**, $[Cu_2(L_3)_2]$ (**3**), $[Cu_2(L_4)_2]$ **4**, and $[Cu_2(L_5)_2]$ **5** were obtained as represented in Scheme 1. All these Schiff base ligands existing with two phenolate oxygen at their terminal phenyl rings and two C=N nitrogens, they possess two bindentate binding domains separated by *m*-xylene spacer moiety. The salicylaldehyde head group in **1** was substituted appropriately by Cl, Br, $OCH_3$, and *t*-butyl in complex **2**–**5**, respectively. Interestingly, though the crystal structures obtained for complexes **1** and **2** supporting the binuclear helical architecture, the UV–Vis and EPR spectral studies carried out for these complexes explored the mononuclear electronic features.

### 3.1. Spectral investigation

The $^1H$ NMR spectra recorded for all five ligands $L_1H_2$–$L_5H_2$ in $CDCl_3$ depicting the characteristic resonance at 8.35–8.46$\delta$, represent the formation of CH=N azomethine group except $L_4H_2$, which did not have azomethine hydrogen. The characteristic IR bands for

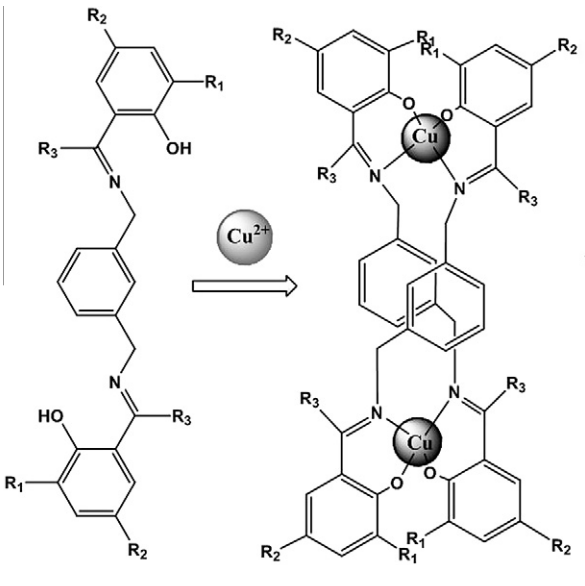

| Ligand | Complex | $R_1$ | $R_2$ | $R_3$ |
|---|---|---|---|---|
| $L_1H_2$ | 1 | H | H | H |
| $L_2H_2$ | 2 | H | Cl | H |
| $L_3H_2$ | 3 | H | Br | H |
| $L_4H_2$ | 4 | $OCH_3$ | H | $CH_3$ |
| $L_5H_2$ | 5 | t-butyl | t-butyl | H |

**Scheme 1.** Synthesis of double stranded $Cu_2$-helical complexes.

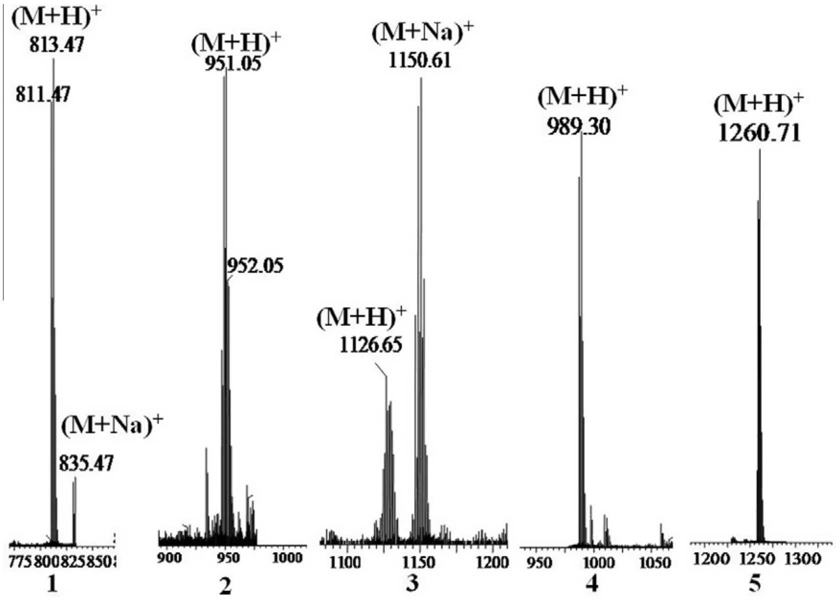

**Fig. 1.** Mass spectra for complexes **1**–**5** recorded in $CH_2Cl_2$:MeOH (50:50 v/v) solvent.

$L_1H_2$–$L_5H_2$ corresponded to (i) OH, (ii) C═N were elicited. The broad signal centered at 3400 $cm^{-1}$ for all these free ligands, can be ascribed to the OH functional group. The sharp and intense peaks in the range of 1510–1517 and 1610–1618 $cm^{-1}$ can be attributed to the $\nu_{CH=N}$ symmetric and *anti*-symmetric stretching mode, respectively, in the case of free ligands. The disappearance of the OH peak and the shift of 10–25 $cm^{-1}$ in the $\nu_{CH=N}$ stretching frequency in IR spectra of these complexes with respect to the corresponding free ligands indicates their complexation with Cu(II) metal center.

The mass spectra obtained for complexes **1**–**5** are depicted in Fig. 1. The mass spectral data showing characteristic positive molecular ion peak, the mass values obtained are in accordance with the formation of dinuclear $Cu_2$ species. Thus an excellent agreement between the experimental and calculated values confirmed the formation of the binuclear double stranded complexes. All these complexes depicting a dominant peak with respect to their monopositive ion $(M+H)^+$, i.e., 811.47 for (**1**), 951.05, (**2**); 1126.65 (**3**); 989.30, (**4**); and 1260.71 for (**5**), the complexes **1** and **3** gave an additional peak correspond to their monopositive sodium ion $(M+Na)^+$ adduct as illustrated in Fig. 1. All these mass spectra thus supported the existence of two metal ions and two ligands without any ambiguity. The bunch of peaks appropriate for the ESI species strongly supports, various isotopic as well as positive ion species, which clearly supports the formation of 2:2 metal ligand dimeric associations. It may be noted that the mass values of complexes with $Na^+$ adduct [complex+$Na^+$] is well-known phenomenon in LC mass spectrometry [34] and hence it is not uncommon.

The dinuclear metal complexes **1**–**5** are found to be dark brown in color and are soluble in $CH_2Cl_2$ and $CHCl_3$. The electronic spectrum for all these complexes behaving quite similar, they exhibit two characteristic bands at 300–330 and 380–420 nm representing various inter and intra ligand transitions as illustrated in Fig. 2. The former band at 300–330 nm can be attributed to $\pi$–$\pi^*$ and n–$\pi^*$ transitions. The band appeared at 380–420 nm can be assigned to the ligand to metal charge transfer of non-bonding lone pair of the phenolate oxygen to the d-orbitals of the Cu(II), i.e., LMCT [35–37]. The broad spectral feature centered at 620–660 nm in the visible region obtained for complexes **1**–**5** can be attributed to the d–d transition. The red shift observed in the $\lambda_{max}$ of UV–Vis spectra arranged in the ascending order **1** (600 nm) < **4** (620 nm) < **2** (620 nm) < **3** (630 nm) < **5** (660 nm) indicate the increasing distortion on the tetrahedrally distorted square planar geometry of the complexes [38,39].

### *3.2. Crystal structure and molecular association*

Our attempt to crystallize all these five complexes was partially successful and we were fortunate to get crystals for complexes **1**–**3**. Though we obtained crystal for complex **3**, our repeated attempts failed to refine the structure and hence we have depicted here only the respective crystallographic data.[1] The complex **1** was crystallized in ethanol, while the complex **2** was obtained from 50:50 solvent mixture of dichloromethane and acetonitrile. Summary of the crystallographic data and selected bond distances, bond angles for complexes **1** and **2** are depicted in Tables 1 and 2, respectively.

Complexes **1** and **2** were crystallized in centrosymmetric space group $P2_1/c$ and $Pbcn$, respectively. An ORTEP view of the neutral Cu(II) complexes **1** and **2** with atom numbering scheme is depicted in Fig. 3. While the complex **1** crystallized with one ethanol molecule, the complex **2** possess no solvent of crystallization. The Cu(II) metal sitting on twofold axis, both the metal centers in the dinuclear unit possess a tetrahedrally distorted square planar geometry coordinating with $N_2O_2$ donor atoms of deprotonated phenolate oxygens and azomethine nitrogens from two different Schiff base ligands in a symmetry related bidentate fashion. The Cu–N distances ranging 1.955–1.958 Å, 1.943–1.970 Å, and the Cu–O distances 1.896–1.916 Å, 1.881–1.891 Å, respectively, in complex **1** and **2**, are well within the range reported for the related Schiff base complexes [40,41]. The *cis*-angles subtended by the six-membered chelate rings with Cu(II) in complexes **1** and **2** from each ligand ranging 88.8–94.2°, 92.2–94.2°, respectively, are within the limit of square planar value. However the *trans*-angles in the range of 152.5–164.3°, 150.7–151.1° are deviated from square planar and

---

[1] *Crystal data for complex **3**:* $C_{44}H_{32}Br_4Cu_2N_4O_4$, formula weight = 1127.45, Orthorhombic, $P2_12_12_1$; $a = 12.7257(16)$, $b = 23.687(3)$, $c = 53.667(7)$ Å, $U = 16177(3)$ Å$^{-3}$, $T = 110(2)$ K, $Z = 4$, $D_c = 1.852$ mg m$^{-3}$, $\mu$(Mo K$\alpha$) = 5.053 mm$^{-1}$, $F(0\,0\,0) = 8864$, $0.11 \times 0.09 \times 0.03$ mm; 98 905 reflections measured of which 37 831 were unique ($R_{int} = 0.1455$), 1049 parameters, $wR_2 = 0.1846$, $R_1 = 0.1013$ (with $I \geqslant 2\sigma(I)$), $S = 1.017$.

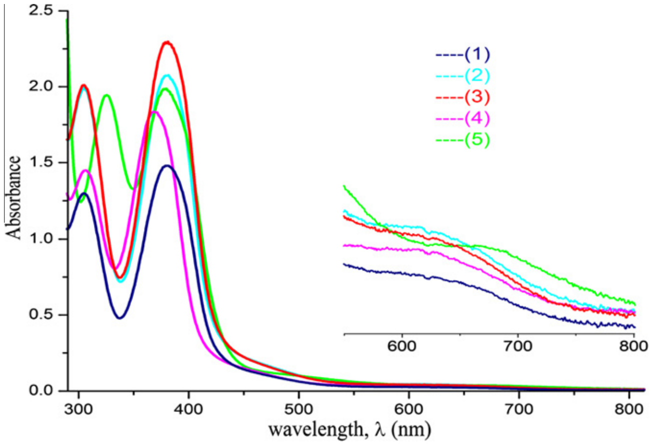

**Fig. 2.** UV Spectrum for **1–5** in $CH_2Cl_2$ (inset shows d–d band).

**Table 1**
Summary of the Crystallographic data for complexes **1** and **2**.

| Parameter | **1** | **2** |
|---|---|---|
| CCDC No. | 773239 | 773240 |
| Formula | $C_{46}H_{42}Cu_2N_4O_5$ | $C_{44}H_{32}Cl_4Cu_2N_4O_4$ |
| $M_W$ | 857.92 | 949.62 |
| Crystal system | monoclinic | orthorhombic |
| Space group | $P2_1/c$ | $Pbcn$ |
| $a$ (Å) | 16.4414(12) | 12.891(12) |
| $b$ (Å) | 9.8667(7) | 13.324(11) |
| $c$ (Å) | 24.3148(18) | 23.68(2) |
| $V$ (Å3) | 3944.1(5) | 4067(6) |
| $Z$ | 4 | 4 |
| $T$ (K) | 100(2) | 293(2) |
| $\mu$(Mo K$\alpha$) (mm$^{-1}$) | 1.131 | 1.358 |
| Reflections measured | 23 306 | 9335 |
| Independent reflections | 9210 [$R_{int}$ = 0.0440] | 2577 [$R_{int}$ = 0.1735] |
| Final $R_1$, $wR_2$ [$I > 2\sigma(I)$] | $R_1$ = 0.0556,<br>$wR_2$ = 0.1179 | $R_1$ = 0.0798,<br>$wR_2$ = 0.1223 |

**Table 2**
Selected bond distances and bond angles for complexes **1** and **2** with esd's are in parentheses.

| Complex **1** | | | |
|---|---|---|---|
| *Bond lengths (Å)* | | | |
| Cu(2)–O(4) | 1.896(2) | Cu(1)–O(3) | 1.906(2) |
| Cu(2)–O(2) | 1.904(2) | Cu(1)–O(1) | 1.916(2) |
| Cu(2)–N(2) | 1.955(2) | Cu(1)–N(3) | 1.955(3) |
| Cu(2)–N(4) | 1.956(2) | Cu(1)–N(1) | 1.958(3) |
| Cu(2)–O(4) | 1.896(2) | Cu(1)–O(3) | 1.906(2) |
| *Bond angles (°)* | | | |
| O(4)–Cu(2)–O(2) | 152.55(10) | O(3)–Cu(1)–O(1) | 155.11(9) |
| O(4)–Cu(2)–N(2) | 90.12(9) | O(3)–Cu(1)–N(3) | 93.29(10) |
| O(2)–Cu(2)–N(2) | 94.28(10) | O(1)–Cu(1)–N(3) | 92.60(9) |
| O(4)–Cu(2)–N(4) | 93.58(9) | N(3)–Cu(1)–N(1) | 164.33(10) |
| O(2)–Cu(2)–N(4) | 91.06(10) | O(1)–Cu(1)–N(1) | 91.97(10) |
| N(2)–Cu(2)–N(4) | 160.87(10) | O(3)–Cu(1)–N(1) | 88.82(10) |
| Complex **2** | | | |
| *Bond lengths (Å)* | | | |
| O(2)–Cu(1)$^{\#1}$ | 1.891(7) | Cu(1)–O(2)$^{\#1}$ | 1.891(7) |
| N(2)–Cu(1)$^{\#1}$ | 1.943(9) | Cu(1)–N(2)$^{\#1}$ | 1.943(9) |
| Cu(1)–O(1) | 1.881(7) | Cu(1)–N(1) | 1.970(9) |
| *Bond angles (°)* | | | |
| O(1)–Cu(1)–O(2)$^{\#1}$ | 150.7(3) | O(2)$^{\#1}$–Cu(1)–N(1) | 92.2(4) |
| O(1)–Cu(1)–N(2)$^{\#1}$ | 94.2(4) | N(2)$^{\#1}$–Cu(1)–N(1) | 151.1(4) |
| O(2)#1–Cu(1)–N(2)$^{\#1}$ | 94.0(4) | | |

$^{\#1}$$-x + 1$, $y$, $-z + 3/2$.

indicate the existence of a tetrahedrally distorted square planar geometry. Each molecule existing in binuclear association, the two symmetrically disposed ligand moieties are wrapped around the M–M axis and generate a dinuclear double helical architecture.

The packing diagram with H-bonding interactions (Supplementary Figs. S1 and S2) indicated that the adjacent molecules, are aligned in layers and are bridged via intermolecular C–H···O [O4···H20–C20 = 3.394 Å] interaction in complex **1** and C–H···Cl [Cl1···H12–C12 = 3.628; ∠Cl1···H12–C12 = 142.21°] contact in **2**. Thus the weak interaction facilitating the formation of a double stranded helical chain, generates "P" and "M" sense of global helicity. Interestingly, the close scrutiny of the crystal structure illustrated that the absolute configuration around the tetrahedrally distorted Cu(II) cations possess opposite chirality, i.e., Delta (Δ) and Lambda (Λ). Further, the ligand wrapping around the "Δ" and "Λ" metal center, the global chirality can be assigned as "P" (*-positive*) and "M" (*-minus*) based on the left and right handed rotation. This unique arrangement can best be described as side-by-side complex [42–45] according to Piguet et al. [9]· while Albrecht [11,46] defines this as mesohelicates.

### 3.3. C–H···π (metal-chelate ring) influenced inter planar twist

The complexes **1** and **2** being helical, the existence of weak CH···π (metal-chelate ring) interaction [47,48] and its influence on shaping the helical conformation is given special attention. Surprisingly, the reports on these class of complexes, though suggest the presence of CH···π and π···π stacking interactions, they mainly focus on the interaction between the phenyl rings. Further, all such contacts exceeding more than 4 Å (weak and long range interaction), they ignored or unnoticed the existence of the CH···π (metal-chelate ring) interaction [49–53]. Thus the present study differing from the previous reports explores the existence of CH···π interaction and its influence on helical conformation.

Both these dinuclear complexes existing in $C_2$ symmetry, they possess four 6-membered metal-chelate rings around the Cu(II) centers. An analysis regarding their contact with neighboring hydrogens was carried out (Supplementary Fig. S3). In this regard the above Scheme 2a and b illustrate the existence of CH···π contact and interplanar twist angle() between the metal-chelate rings, respectively. To simplify the understanding, the centroids of all these four 6-membered chelate rings are assigned as $Cg^a$, $Cg^{a'}$, $Cg^b$, $Cg^{b'}$ as shown in Scheme 2a. The phenyl rings of the *m*-xylene spacer on the opposite strands are staggered with each other and the respective mean planes measured in complex **1** and **2** are found to be 34.5° and 32.0°. The hydrogens of *m*-xylene spacer are found to be under the influence of the metal-chelate rings, as reflected from their respective C–H···π distances (Table 3).

Based on the H-bonding distances, it is obvious that the hydrogens H12 [H12···$Cg^{b'}$ = 3.00Å] and H14[$Cg^a$···H14 = 3.42 Å] of *m*-xylene in **1** are shorter than that of the respective hydrogens H32 and H36 from the opposite strand. A similar approach in complex **2** produced only two set of identical C–H···π contacts, due to its crystallographic symmetry. The H10 of the *m*-xylene ring belong to opposite strands, possess a stronger contact with $Cg^b$ and $Cg^{b'}$ [H10···$Cg^{b/b'}$ = 2.64 Å], while the H14 possess comparatively weaker contact with the $Cg^a$ and $Cg^{a'}$ [H14···$Cg^a$/$Cg^{a'}$ = 3.38 Å].

In complex **1**, one of the *m*-xylene spacer was dragged towards the metal-chelate ring $Cg^a$ and $Cg^{b'}$ through its hydrogens H14 and H12, respectively. Similarly the other *m*-xylene spacer with H32 and H36 resides away, i.e., >3.7 Å. However a similar interaction in complex **2** defined by H10 established a stronger influence with the respective metal-chelate rings $Cg^b$ and $Cg^{b'}$. Both these complexes exploring the existence of C–H···π (metal-chelate ring) contacts [54–57] with opposite strands, this analysis further strengthens their influence on shaping the helical conformation.

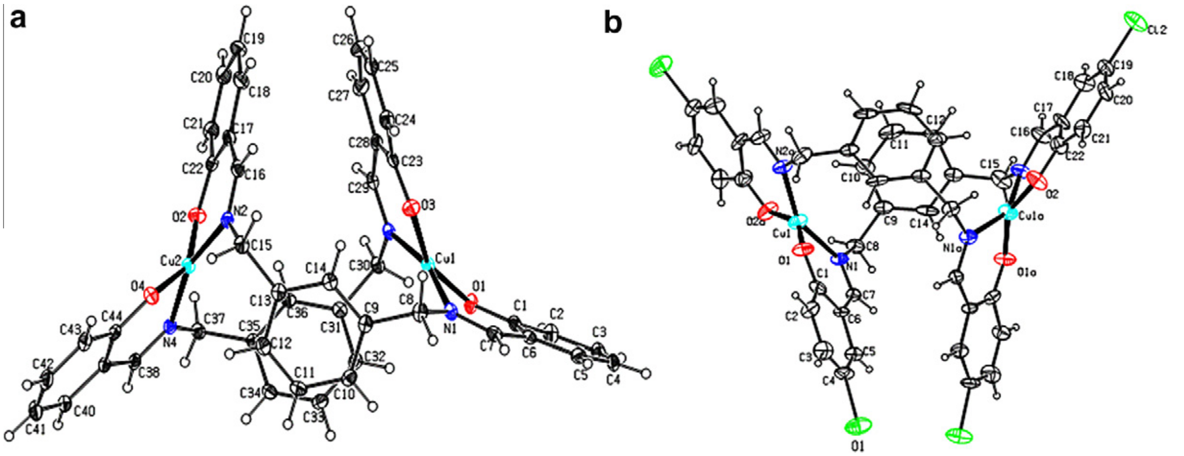

**Fig. 3.** ORTEP diagram depicting the complex (a) $[Cu_2(L_1)_2]\cdot EtOH$ (**1**), (b) $[Cu_2(L_1)_2]$ (**2**) with atom numbering scheme (40% probability factor for the thermal ellipsoid).

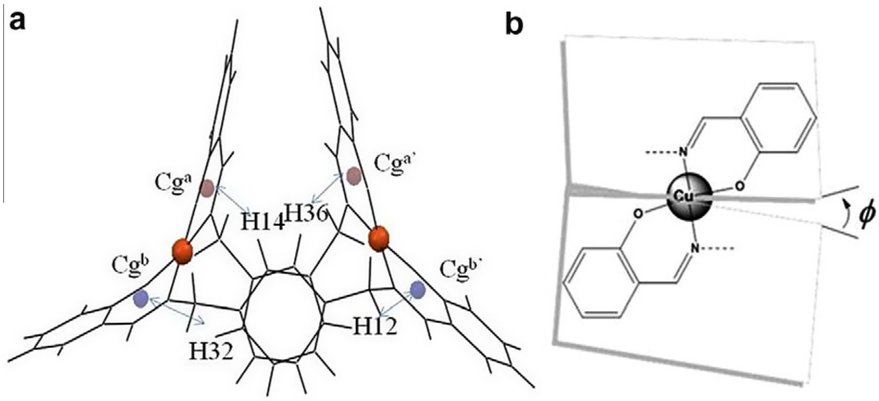

**Scheme 2.** (a) Centroid assignment for all chelate rings. (b) Interplanar twist angle.

**Table 3**
$CH\cdots\pi$ contact measured in complexes **1** and **2**.

| D–H···A | Dist (Å) | H···A | Dist. (Å) | ∠D–H···A | Angle (°) |
|---|---|---|---|---|---|
| *Complex **1*** | | | | | |
| C14–H14···$Cg^{a}$ | 3.78 | H14···$Cg^{a}$ | 3.42 | ∠C14H14···$Cg^{a}$ | 105.7 |
| C32–H32···$Cg^{b}$ | 4.08 | H32···$Cg^{b}$ | 3.36 | ∠C32H32···$Cg^{b}$ | 135.9 |
| C36–H36···$Cg^{a\prime}$ | 3.98 | H36···$Cg^{a\prime}$ | 3.62 | ∠C36H36···$Cg^{a\prime}$ | 106.0 |
| C12–H12···$Cg^{b\prime}$ | 3.78 | H12···$Cg^{b\prime}$ | 3.00 | ∠C12-H12···$Cg^{b\prime}$ | 139.0 |
| *Complex **2*** | | | | | |
| C14–H14···$Cg^{a}/C_{g}^{a\prime}$ | 3.80 | H14···$Cg^{a}$ | 3.38 | ∠C14-H14···$Cg^{a}$/ $C_{g}^{a\prime}$ | 110.1 |
| C10–H10···$Cg^{b}/Cg^{b\prime}$ | 3.45 | H10···$Cg^{b}$ | 2.64 | ∠C10-H10···$Cg^{b}$/ $Cg^{b\prime}$ | 145.7 |

The six membered chelate rings existing with nitrogen and oxygen atoms, which possess unpaired electrons may gain electron delocalization. The electron delocalization might have given the nucleophilic nature and hence they tend to have contact with electrophilic hydrogen of *m*-xylene spacer. The weak supramolecular interaction between the *m*-xylene hydrogen and the metal-chelate ring, thus, found varied depending upon their proximity. Depending upon the strength of the $CH\cdots\pi$ interaction, the metal chelate rings may not be possible to retain their planarity. Accordingly an interplanar twist measured between the metal-chelate rings gives the possibility for the formation of square planar or tetrahedral geometry at Cu(II). Based on the classical method [58–61], the interplanar twist angle ($\phi$) (Scheme 2b) 0, 180° defines square planar geometry, while 90° defines the tetrahedral geometry. The interplanar angle in complex **1** with 41.5° at Cu(1) and 44.8° at Cu(2), and the Cu center in complex **2** exists with 44.0° undoubtedly support the existence of an intermediate geometry between the square planar and tetrahedral thus leading to a tetrahedrally distorted square planar geometry.

### 3.4. EPR spectral investigation

The complexes **1**–**5** were characteristically binuclear, which inspired us to investigate their M–M interaction. Accordingly the X-band EPR spectra [62–66] of polycrystalline powder at room temperature for complexes **2**, **3**, and **5** were recorded (Fig. 4). All these spectra showing similar spectral pattern, their broad feature could be attributed to the dipolar interaction. The position of the EPR signal and the absence of $\Delta Ms = \pm 1$ resonance strongly suggested, that the molecules though assembled binuclear in nature, they still possess a non-interacting M–M association. The Cu–Cu distances measured as 6.377 and 6.591 Å, respectively, from the crystal structures of **1** and **2**, also supports the possibility of the existence of non-interacting Cu(II) centers.

### 3.5. Catalytic studies

Copper(II) complexes with four-coordination can generally exist in distorted square-planar or tetrahedral geometry. However on comparison with square planar, the tetrahedral geometry was relatively rare, while it was very common for Cu(I) complexes. The

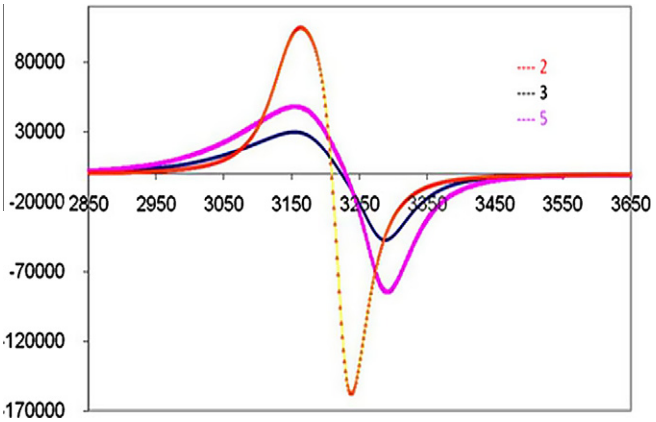

**Fig. 4.** X-band spectra at 298 K of powder samples of complexes **2**, **3**, and **5**.

present complexes with Cu(II) active sites existing in tetrahedrally distorted square planar geometry, the helical architecture gains added importance. Hence they were chosen for their catalytic activity. In this study, we have carried out Henry reaction (Fig. 5) using complex **5** as representative catalyst with 4-nitrobenzaldehyde as substrate in presence of nitromethane. In order to obtain highest yield of the product nitroalcohol, an optimization of the reaction conditions was carried out, varying the catalyst loading, temperature etc through a series of experiments and the results are presented in Table 4.

On increasing the catalyst loading from 5 to 30 mol% at 70 °C in THF (Entry 1–4) we found that 20 mol% catalyst loading at 70 °C (Entry 3) was optimum for achieving high yield (up to 85% from 48%) of corresponding nitroalcohol in 35 h. As temperature and solvents played a crucial role for the catalytic reaction, the Henry reaction was conducted at different temperatures, i.e., rt, 50, 70, and 75 °C. Therefore on conducting the Henry reaction upon decreasing the temperature from 70 °C to rt, the yield of nitroalcohol was adversely affected (Entries 5 and 6). However on increasing the temperature from 70 to 75 °C (Entry 7) there was no improvement in the product yield. Further attempts were made to see the effect of solvents such as THF, $CHCl_3$, $CH_2Cl_2$ (Entries 3, 8, and 9) on Henry reaction [67]. Among all the solvents used for this study, THF was found to be the solvent of choice (Entry 3), while the other two solvents were not found encouraging. Under this optimized reaction conditions (Entry 3), the reaction was also carried out with 2-flurobenzaldehyde as substrate, where 75% yield (Entry 10) of corresponding nitroalcohol was obtained. A blank reaction was conducted in the absence of catalyst **5** using 4-nitrobenzaldehyde as substrate in presence of nitromethane at 70 °C, where only trace quantity of nitroalcohol was obtained (Entry 11). To confirm the role of the counter ions in the catalyst **5**, nitroaldol reaction was carried out with 4-nitrobenzaldehyde as substrate in presence of nitromethane at 70 °C using copper(II)triflate and copper(I)iodide in place of copper(II)acetate. However, the results are not encouraging in terms of yield of nitroalcohol (yield <10%). As all these five helicates were possessing almost very similar stereochemical structure, we have chosen the complex **5** for this catalytic study, since such sterically strained complexes were demonstrated for better catalytic capability.

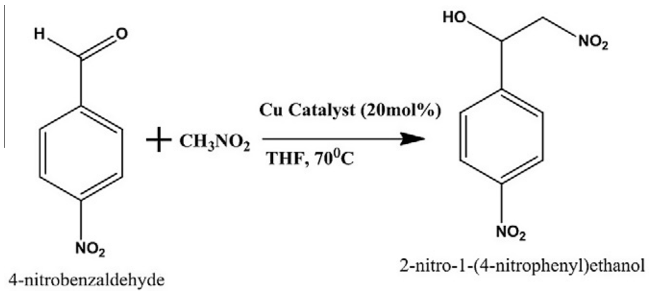

**Fig. 5.** Henry reaction followed for complex **5** as catalyst.

**Table 4**
The catalytic activity of **5** in Henry reaction of 4-nitro benzaldehyde and nitro methane.

| Entry | Catalyst (mol%) | Temp. (°C) | Solvent | Time (h) | Yield (%) |
|---|---|---|---|---|---|
| 1 | 5 | 70 | THF | 35(48) | 48 |
| 2 | 10 | 70 | THF | 35(48) | 72 |
| 3 | 20 | 70 | THF | 35(48) | 85 |
| 4 | 30 | 70 | THF | 35(48) | 85 |
| 5 | 20 | 50 | THF | 48 | 65 |
| 6 | 20 | RT | THF | 48 | 45 |
| 7 | 20 | 75 | THF | 35(48) | 85 |
| 8 | 20 | 45 | DCM | 35 | 35 |
| 9 | 20 | 60 | $CHCl_3$ | 35 | 40 |
| 10[a] | 20 | 70 | THF | 35(48) | 75 |
| 11 | – | 70 | THF | 48 | Trace |

[a] 2-Flouro benzaldehyde as substrate.

The metal-chelate ring existing with nucleophilic nature, it possesses strong contact with *m*-xylene ring hydrogen as demonstrated in the crystal structure. A similar situation may arise, when the substrate nitromethane approach the catalyst **5**. It is expected that the hydrogen bonding contact with *m*-xylene hydrogen will be weakened, when comparatively a stronger electrophile comes into contact. Thus the nitromethane certainly being stronger electrophile compared to the hydrogen of *m*-xylene ring, we propose [68–72] that the removal of hydrogen from nitromethane would be facilitated by the nucleophilic attack on aldehydic carbon giving the nitroalcohol as an end product as shown in Scheme 3. In general, researchers [73] use triethylamine to facilitate the deprotonation of nitromethane during the course of the catalytic reaction. However, in the present case since the complex **5** itself performing the deprotonation, this can be considered as an added advantage of the catalyst.

## 4. Conclusions

In summary, we have synthesized a series of dinuclear $Cu_2$ "metallohelicate" complexes, which retained the tetrahedrally distorted square planar geometry. All these bis-bidentate Schiff base ligands with *m*-xylene spacer possess two well separated binding domains and formed stereochemically important Cu(II) binuclear helicates is illustrated from the crystal structure. The crystal structures obtained for complexes **1** and **2** showing the helical architecture, the influence of $CH\cdots\pi$ metal-chelate ring interaction and the analysis on their consequent geometrical change demonstrate the stabilization of tetrahedrally distorted square planar geometry at Cu(II) metal center without any ambiguity. The tetrahedrally distorted square planar Cu(II) in the binuclear association possess both the $\Delta$ and $\Lambda$ chirality, and the ligand wrapped around the dimetallic association generates both ***P*** and ***M*** chirality which result the complexes as mesocates in every form. The $CH\cdots\pi$ contact in complex **1** being weak and long range, the respective interaction in complex **2** was found strong. This supramolecular interaction thus unequivocally established its influence in framing the helical conformation and the geometrical rearrangement. The EPR spectra obtained for complexes **2**, **3**, and **5** indicated that though the binuclear association existed in the helicate, both these metal ions were isolated significantly from each other and possess a non-interacting M–M association. The catalytic activity performed following

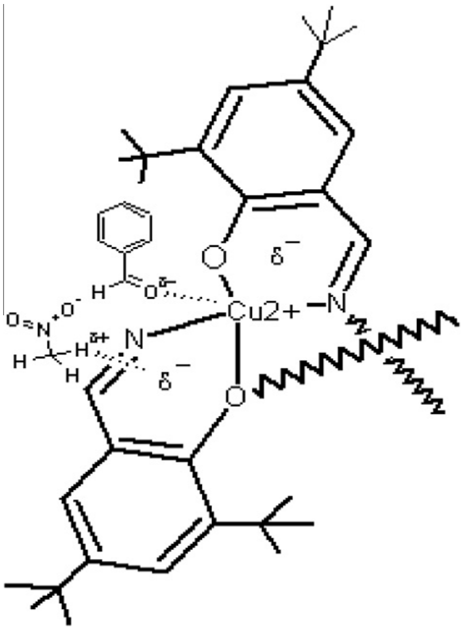

**Scheme 3.** Proposed mechanism for nitroaldol reaction.

Henry reaction by complex **5** catalyzing the 4-nitrobenzaldehyde to the corresponding nitroalcohol gave 85% yield at 70 °C and suggested that these complexes can be used as catalyst for such nitroaldol reactions.

## Acknowledgements

The authors P.S., P.M.S. and S.N. gratefully acknowledge the financial support extended by DST (Project No. SR/S1/IC-19/2005) and CSIR New Delhi (NWP 0010). Mr. Arun Kumar Das and Mr. Vinod Agarwal are gratefully acknowledged for recording MS and IR spectra, respectively.

## Appendix A. Supplementary material

CCDC Nos. 773239 and 773240 for complexes **1** and **2** contains the supplementary crystallographic data for this paper. These data can be obtained free of charge from The Cambridge Crystallographic Data Centre via www.ccdc.cam.ac.uk/data_request/cif.

Supplementary data associated with this article can be found, in the online version, at doi:10.1016/j.ica.2011.04.033.

## References

[1] K.W. Penfield, R.R. Gay, R.S. Himmelwright, N.C. Eickman, V.A. Norris, H.C. Freeman, E.I. Solomon, J. Am. Chem. Soc. 103 (1981) 4382.
[2] E.I. Solomon, K.W. Penfield, D.E. Wilcox, Struct. Bonding 53 (1983) 1.
[3] B.J. Hathaway, in: G. Wilkinson, R.D. Gillard, J.A. McCleverty (Eds.), Comprehensive Coordination Chemistry, vol. 5, Pergamon Press, Oxford, 1987, p. 558 (Chapter 53).
[4] A. Messerschmidt, Adv. Inorg. Chem. 40 (1994) 121.
[5] A.G. Sykes, Adv. Inorg. Chem. 36 (1991) 377.
[6] C.R. Jacob, S.P. Varkey, P. Ratnasamy, Microporous Mesoporous Mater. 22 (1998) 465.
[7] C.R. Jacob, S.P. Varkey, P. Ratnasamy, Appl. Catal. A 168 (1998) 353.
[8] J.M. Lehn, Supramolecular Chemistry. Concepts and Perspectives, VCH, Weinheim, 1995.
[9] C. Piguet, G. Bernardinelli, G. Hopfgartner, Chem. Rev. 97 (1997) 2005.
[10] E.L. Eliel, S.H. Wilen, L.N. Mander, Stereochemistry of Organic Compounds, Wiley, New York, 1994 (Chapter 4).
[11] M. Albrecht, Chem. Rev. 101 (2001) 3457.
[12] M.J. Hannon, L.J. Childs, Supramol. Chem. 16 (2004) 7.
[13] H. Jiang, A. Hu, W. Lin, Chem. Commun. 961 (2003) 961.
[14] H.-L. Kwong, H.-L. Yeung, W.-S. Lee, W.-T. Wong, Chem. Commun. (2006) 4841.
[15] N. Yoshida, H. Oshio, T. Ito, Chem. Commun. (1998) 63.
[16] N. Yoshida, H. Oshio, T. Ito, J. Chem. Soc., Perkin Trans. 2 (1999) 975.
[17] B.J. McNelis, L.C. Nathan, C.J. Clark, J. Chem. Soc., Dalton Trans. (1999) 1831.
[18] Y. Song, I.A. Koval, P. Gamez, G.A. Van Albada, I. Mutikainen, U. Turpeinen, J. Reedijk, Polyhedron 23 (2004) 1769.
[19] K.T. Potts, K.M. Kesharvarzz, F.K. Tham, H.D. Abruna, C. Arana, Inorg. Chem. 32 (1993) 4422.
[20] K.T. Potts, K.M. Kesharvarzz, F.K. Tham, H.D. Abruna, C. Arana, Inorg. Chem. 32 (1993) 4436.
[21] K.T. Potts, C.P. Horwitz, A. Fessak, K.M. Keshavarz, K.E. Nash, P.J. Toscano, J. Am. Chem. Soc. 115 (1993) 10444.
[22] E.C. Constable, T. Kulke, M. Neuburger, M. Zehnder, Chem. Commun. (1997) 489.
[23] E.C. Constable, M.G.B. Drew, M.D. Ward, J. Chem. Soc., Chem. Commun. (1987) 1600.
[24] M. Barely, E.C. Constable, S.A. Corr, M.G.B. Drew, R.C.S. McQueen, J.C. Nutkins, M.D. Ward, J. Chem. Soc., Dalton Trans. (1988) 2655.
[25] R. Kramer, J.-M. Lehn, A. Marquis-Rigault, Proc. Natl. Acad. Sci. USA 90 (1993) 5394.
[26] C.M.V. Smith, J.-M. Lehn, Chem. Commun. (1996) 2735.
[27] F.A. Luzzio, Tetrahedron 57 (2001) 915.
[28] G.M. Sheldrick, SAINT, 5.1 ed., Siemens Industrial Automation Inc., Madison, WI, 1995.
[29] SADABS, Empirical absorption Correction Program, University of Göttingen, Göttingen, Germany, 1997.
[30] G.M. Sheldrick, Acta Crystallogr., Sect. A 46 (1990) 467.
[31] G.M. Sheldrick, Acta Crystallogr., Sect. A 64 (2008) 112.
[32] A.L. Spek, PLATON-97, University of Utrecht, Utrecht, The Netherlands, 1997.
[33] Mercury 1.3 Supplied with Cambridge Structural Database, CCDC, Cambridge, UK, 2003–2004.
[34] S. Patra, P. Paul, Dalton Trans. (2009) 8683.
[35] H. Colchoubian, W.L. Waltz, J.W. Quail, Can. J. Chem. 77 (1999) 37.
[36] C. Fraser, B. Bosnich, Inorg. Chem. 33 (1994) 338.
[37] M. Vilas-Boas, C. Freire, B. Castro, P.A. Chistensen, A.R. Hillman, Inorg. Chem. 36 (1997) 4919.
[38] E.I. Solomon, M.J. Baldwin, M.D. Lowery, Chem. Rev. 92 (1992) 521.
[39] R.I. Harlow, W.J. Wells, S.H. Simonsons, Inorg. Chem. 14 (1975) 1768.
[40] M.M. Bhadbhade, D. Srinivas, Inorg. Chem. 32 (1993) 5458.
[41] E. Suresh, M.M. Bhadbhade, D. Srinivas, Polyhedron 15 (1996) 4133.
[42] C.O. Dietrich-Buchecker, J.F. Nierengarten, J.P. Sauvage, N. Armaroli, V. Balzani, I. De Cola, J. Am. Chem. Soc. 115 (1993) 11237.
[43] W. Zarges, J. Hall, J.-M. Lehn, C. Bolm, Helv. Chim. Acta 74 (1991) 1843.
[44] C. Piguet, G. Hopfgartner, B. Bocquet, O. Schaad, A.F. Williams, J. Am. Chem. Soc. 116 (1994) 9092.
[45] J. Xu, T.N. Parac, K.N. Raymond, Angew. Chem., Int. Ed. 38 (1999) 2878.
[46] M. Albrecht, Chem. Eur. J. 6 (2000) 3485.
[47] D. Sredojevic, G.A. Bogdanovic, Z.D. Tomic, S.D. Zaric, Cryst. Eng. Commun. 9 (2007) 793.
[48] B. Manimaran, L.-J. Lai, P. Thanasekaran, J.-Y. Wu, R.-T. Liao, J.-W. Tseng, Y.-H. Liu, G.-H. Lee, S.-M. Peng, K.-L. Lu, Inorg. Chem. 45 (2006) 8070.
[49] P. Mosae Selvakumar, E. Suresh, P.S. Subramanian, Polyhedron 28 (2009) 245.
[50] U. Mukhopadhyay, D. Choquesillo-Lazarte, J. Niclos-Gutierrez, I. Bernal, Cryst. Eng. Commun. 6 (2004) 627.
[51] Z.D. Tomic, V.M. Leovac, Z.K. Jacimovic, G. Giester, S.D. Zaric, Inorg. Chem. Commun. 9 (2006) 833.
[52] Z.D. Tomic, S.B. Novakovic, S.D. Zaric, Eur. J. Inorg. Chem. (2004) 2215.
[53] Z.D. Tomic, D. Sredojevic, S.D. Zaric, Cryst. Growth Des. 6 (2006) 290.
[54] M. Nishio, M. Hirota, Y. Umezawa, The C–H$\cdots\pi$ Interaction (Evidence, Nature and Consequences), Wiley-VCH, New York, 1998.
[55] G.R. Desiraju, T. Steiner, The Weak Hydrogen Bond in Structural Chemistry and Biology, Oxford University Press Inc., New York, 1999.
[56] G.R. Desiraju, Acc. Chem. Res. (2002) 565.
[57] M. Barcelo-Oliver, A. Terron, A. Garcia-Raso, N. Lah, I. Turel, Acta Crystallogr., Sect. C 66 (2010) o313.
[58] T.G. Fawcett, S.M. Rudich, B.H. Toby, R.A. Lalancette, J.A. Potenza, H.J. Schugar, Inorg. Chem. 19 (1980) 940.
[59] M.N. Potenza, J.A. Potenza, H.J. Schugar, Acta Crystallogr., Sect. C 44 (1988) 1201.
[60] P.J. Burke, D.R. McMillin, W.R. Robinson, Inorg. Chem. 19 (1980) 1211.
[61] M. Konda, Y. Shibuya, K. Nabari, M. Miyazawa, S. Yasue, K. Maeda, F. Uchida, Inorg. Chem. Commun. 10 (2007) 1311.
[62] B. Bleaney, K.D. Bowers, Proc. R. Soc. Lond. A 214 (1952) 451.
[63] H. Abe, J. Shimada, Phys. Rev. 90 (1953) 316.
[64] A. Bertini, D. Gatteschi, EPR of Exchange Coupled Systems, Springer-Verlag, Berlin, 1990 (Chapter 10).
[65] S. Chavan, D. Srinivas, P. Ratnasamy, J. Catal. 192 (2000) 286.
[66] J.R. Wasson, C.-I. Shyr, C. Trapp, Inorg. Chem. 7 (1968) 469.
[67] F.A. Luzzio, R.W. Fitch, Tetrahedron Lett. 35 (1994) 6013.
[68] D.A. Evans, D. Seidel, M. Rueping, H.W. Lam, J.T. Shaw, C.W. Downey, J. Am. Chem. Soc. 125 (2003) 12692.
[69] K. Ma, J. You, Chem. Eur. J. 13 (2007) 1863.
[70] G. Zhang, E. Yashima, W.-D. Woggon, Adv. Synth. Catal. 351 (2009) 1255.
[71] B. Qin, X. Xiao, X. Liu, J. Huang, Y. Wen, X.J. Feng, Org. Chem. 72 (2007) 9323.
[72] C. Palomo, M. Oiarbide, A. Laso, Eur. J. Org. Chem. (2007) 2561.
[73] A. Noole, K. Lippur, A. Metsala, M. Lopp, T. Kanger, J. Org. Chem. 75 (2010) 1313.